Journal of the European Ceramic Society 19 (1999) 2511–2517

PII: S0955-2219(99)00103-X
0955-2219/99/$ - see front matter

Residual Stresses in Alumina–Zirconia Laminates

David J. Green,* Peter Z. Cai and Gary L. Messing

Department of Materials Science and Engineering, The Pennsylvania State University, University Park, PA 16802, USA

Abstract

Significant residual stresses can arise in hybrid ceramic laminates during the densification and cooling processing cycles. The densification stresses in alumina–zirconia laminates were calculated assuming the layers to be linear viscous with data obtained by cyclic loading dilatometry. These stresses placed the zirconia layers in biaxial tension and even at 1 MPa or less, they were sufficient to cause a type of linear cavitation damage. The methodology was also applied to asymmetric laminates, successfully predicting their observed curling behaviour. Thermal expansion mismatch stresses arise during cooling, again placing the zirconia layers in residual biaxial tension and leading to the formation of transverse (channelling) cracks. The stresses were calculated using both elastic and viscoelastic formulations and were confirmed with indentation measurements. Additions of alumina to the zirconia layers were effective in reducing both sources of residual stress and allowed crack formation during processing to be avoided. Residual stresses were also shown to improve mechanical performance. © *1999 Elsevier Science Ltd. All rights reserved.*

Keywords: residual stresses, laminates, thermal expansion, Al_2O_3, ZrO_2.

1 Introduction

Hybrid ceramic laminates, which are composed of alternating layers of two or more different ceramic materials, have emerged recently as a viable alternative to fibre-reinforced ceramic composites for structural applications. Fabrication of laminated structures usually employs relatively low-cost conventional processing routes, such as tape casting, sequential slip casting, coating techniques, etc. The processing and mechanical behaviour of laminates has been recently reviewed by Chan.[1] Various toughening mechanisms are available in these laminates. Some workers have emphasized the use of a low fracture energy interface between the layers to deflect cracks, similar to fibre reinforced ceramic composites.[2] In other cases, it appears the changes in elastic modulus, fracture toughness and residual stresses between the layers can play a role in the toughness and strength behaviour.[3–10] In transforming ceramics, the presence of the layers can influence the transformation zone size[11] and in ceramic–metal laminates, crack bridging effects can be important.[12]

A particular challenge in the processing of ceramic laminates is to understand the nature of the residual stresses, particularly if they are to be used to enhance the mechanical properties. Invariably, the materials chosen for the layers will possess different sintering and thermal expansion strains. Thus, one expects that residual stresses will arise both in heating, when the laminate is first densified (differential densification), and in cooling as the layers contract (thermal expansion mismatch). The differential densification will place the layers in either biaxial tension or compression, leading to inhibition or enhancement of the densification. The tensile stresses can be particularly troublesome as they can give rise to 'sintering' cracks.[13] During cooling, the residual stresses can also lead to cracking and three primary crack morphologies have been observed: transverse, longitudinal and debond cracks. Transverse (channelling) cracks form as a result of the in-plane tensile stresses whereas longitudinal surface cracks form in the 'compressed' layer because of the tensile stresses that arise at its free surfaces.[13–15] Transverse and 'edge-effect' cracking can be prevented if the thickness of the 'tensile' layer is reduced below a critical value.[14,15] Alternatively, the critical thickness can be increased by reducing the residual stress or increasing the fracture toughness of the layers.

This paper reviews a series of recent papers that studied the residual stresses that arise in alumina-zirconia laminates during processing and the role these stresses play in the mechanical performance.[16–18] Residual stresses have been observed previously in Al_2O_3–ZrO_2 trilayers and multilayers.[5–9] Yttergren *et al.*[5] have shown that the presence of compressive residual stresses on the surface gives rise to higher values of strength and post-indentation strength over the monolithic

* To whom correspondence should be addressed.

counterparts. The overall approach in the work being reviewed here, was to measure the parameters that control residual stress and then perform theoretical calculations to determine their magnitude. The stress values were then verified by independent means. The residual stresses were also linked to the observed types of processing damage and to the mechanical performance of the laminates.

2 Overview of Experimental Procedure

The starting powders for this work were an MgO-doped Al_2O_3 powder (Premalox, Alcoa) and a CeO_2-stabilized ZrO_2 powder (TZ-12Ce, Tosoh), both with particle sizes in the range of 0·2–0·3 μm. The layers were produced by tape casting, punched into rectangles and formed into green bodies by thermal lamination to form symmetric and asymmetric laminates. The asymmetric laminates curl during firing as a result of the differential shrinkage. Measurement of the curvature change was employed as an indirect confirmation of the theoretical approach used for calculating the differential shrinkage stresses in the symmetric laminates. In the symmetric laminates, the Al_2O_3 and ZrO_2 rectangles were stacked in an alternating sequence to a total of 23 layers, with both of the surface layers being Al_2O_3. In the asymmetric laminates, three Al_2O_3 layers were on one side and three ZrO_2 layers were on the other, forming a laminate resembling a bilayer. In addition to the laminates made of alumina (A100) and zirconia (Z100) layers, symmetric and asymmetric laminates were fabricated in which the compositions of the Z100 layers were modified by adding 10, 20 and 30 wt% alumina. These are denoted as Z90, Z80 and Z70 layers, respectively. Thus, a total of four ZrO_2-containing layers were used to form four types of laminates: A100-Z100, A100-Z90, A100-Z80, and A100-Z70. The addition of Al_2O_3 to the ZrO_2 layers was used to examine the effect of changing the sintering shrinkage and thermal expansion mismatch between the layers.

After a binder burnout cycle, most laminates were subjected to a single firing cycle. The laminates were heated at 5°C min, sintered at 1530°C for 90 min and were cooled at 3°C min. The asymmetric laminates were sintered in a tube furnace for in-situ observation of the curling that occurs during sintering.[16] The difference in densification rates between the layers led to curvature development at about 1000°C and the curvature was measured from photographs taken at 50°C intervals. The complete details of the processing and microstructural characterization are available elsewhere.[16] Residual stress in the outer alumina layers of the symmetric laminates was determined from indentation crack length measurements.[18]

The strength and post-indentation strength of the as-processed symmetric laminates was determined using four-point bending. The details of the mechanical characterization are available elsewhere.[18]

3 Densification Stresses

Figure 1 shows the linear shrinkage curves for monoliths of some of the layer compositions.[16] There is a significant mismatch in the sintering strains for the unconstrained layers of alumina (A100) and zirconia (Z100). The addition of 30 wt% alumina (Z70) clearly decreased the mismatch in sintering strain and strain rate.

Bordia and Scherer[19] contend a simple linear viscous constitutive relationship is sufficient to model the mechanical response of a sintering compact. This is consistent with models for diffusional creep which yield a linear correlation between stress and strain rate. This is also an attractive suggestion as viscoelastic models can be cumbersome or even intractable and difficult to modify for porosity changes. Viscous behaviour also implies that densification stresses in symmetric laminates will depend primarily on the mismatch in sintering strain rate. To determine the viscosity of the layers, cyclic loading dilatometry was used.[20] In this technique, a cyclic stress is applied to a compact as it is heated and densified in a dilatometer. Figure 2 shows an example of such data for alumina as it approaches the maximum sintering temperature. The shaded bars represent the periods when the stress is applied. The stress application leads to change in strain rate and elastic strains are not detected, in line with the proposed viscous behaviour. It is also interesting to note that the compact tends to 'recover' slightly when the stress is

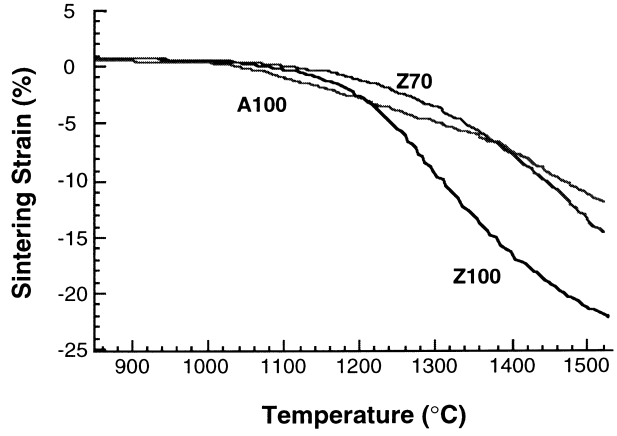

Fig. 1. Linear sintering shrinkage strains for A100, Z100 and Z70 specimens.

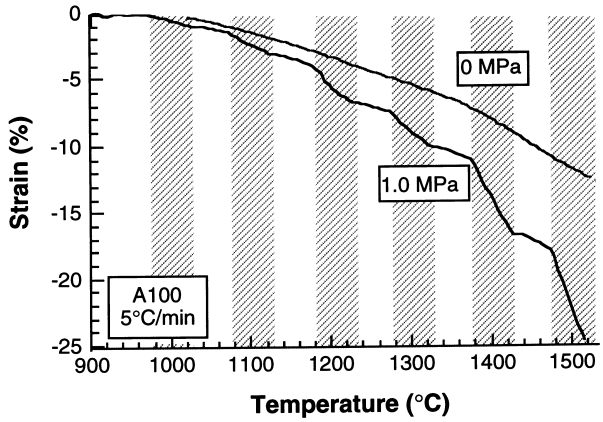

2. Linear shrinkage strain between 900 and 1500 °C for alumina (A100) using thermomechanical analyzer.

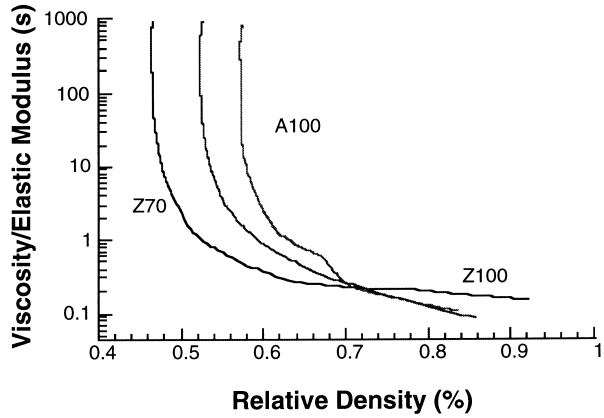

Fig. 4. Measured viscosity-to-elasticity ratio (relaxation time)

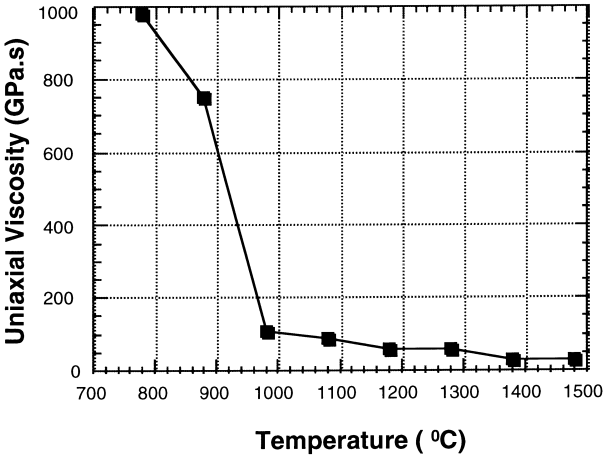

Fig. 3. Calculated uniaxial viscosity as a function of temperature for alumina.

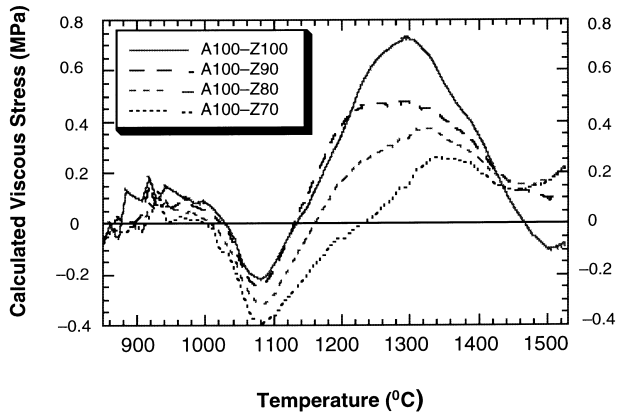

Fig. 5. Layer sintering mismatch stresses in the ZrO_2 layer for the A100–Z100, A100–Z90, A100–Z80 and A100–Z70 symmetric laminates calculated from the mismatch in sintering strain rate.

removed with the strain rate being lower than the stress-free value. By measuring the strain rate for various stresses, viscosity can be determined throughout the densification process. Figure 3 shows the viscosity for the densifying alumina as a function of temperature. A rapid decrease in viscosity is observed for temperatures above ~950°C. It is also useful to determine the viscosity–Young's modulus ratio, i.e., the relaxation time for a Maxwell viscoelastic model. The Young's modulus, E, was determined as a function of the relative density, ρ, using[21,22]

$$\frac{E - E_g}{E_0 - E_g} = \frac{\rho - \rho_g}{1 - \rho_g} \tag{1}$$

where E_g and E_0 are the Young's moduli at the onset of densification and at theoretical density, respectively, and ρ_g is the relative density of the green body. The relaxation time data are shown in Fig. 4 . For a heating rate of 5°C min, one would expect relaxation times less than 10 s would be sufficient to allow the body to behave essentially in a viscous fashion. From Fig. 4, one notes there is a fairly sharp transition from elastic to viscous behaviour. In a symmetric laminate with alternating layers (subscripts 1 and 2), the stress can be calculated for elastic layers using[13]

$$\sigma_1 = \left(\frac{1}{1 + mn}\right)\left(\frac{E_1}{1 - \upsilon_1}\right)\Delta e \tag{2}$$

where

$$m = \frac{h_1}{h_2} \text{ and } n = \left(\frac{E_1}{1 - \upsilon_1}\right)\left(\frac{1 - \upsilon_2}{E_2}\right) \tag{3}$$

h is the layer thickness, E is Young's modulus, υ is Poisson's ratio and Δe is the (unconstrained) mismatch strain. Using the analogy between Hooke's Law (linear elasticity) and Newton's Law (linear viscosity), the stresses in viscous layers can also be calculated from eqns (2) and (3) with E becoming uniaxial viscosity, υ the Poisson's ratio for the viscous material and Δe the mismatch in strain *rate*. An example of the densification stress calculation is shown in Fig. 5 for the zirconia layers, which are subjected primarily to biaxial tensile stresses during densification. The maximum stress occurs at ~1300°C but the magnitudes are < 1 MPa. The data primarily reflect the mismatches in *strain rate* for the

unconstrained layers.[16] The addition of the zirconia to the alumina layers is found to reduce these stresses.

A more complete viscoelastic treatment was also performed for these laminates[17] but this analysis only changed the stresses at temperatures $< 500°C$. Further refinements were also made to determine how the residual stresses change the in-plane densification behaviour [17] but this led to only modest increases in stress. This small effect is a result of two competing effects in which, for example, the increase in viscosity from the densification in the compressive layers is offset to a large degree by the decrease in the driving force for sintering caused by the densification. Figure 6 shows the final results of the more complete viscoelastic calculations.[17] Interestingly, it was predicted that residual stresses may also occur at the maximum sintering temperature but the bodies will be more coherent in this final densification stage.

The densification stresses calculated above are low but are close enough to the sintering stress that de-sintering or other damage mechanisms may be possible.[17] Microstructural observations after laminate processing identified linear arrays of voids in the zirconia layer and these voids appeared to be nucleation sites for the transverse cracks that formed for some of the laminates during cooling.[16] These pores are similar to the creep cavitation damage observed in ceramics. In a separate set of experiments,[23] alumina tapes were formed into uniaxial tensile specimens. These specimens were then subjected to stresses up to 2 MPa, while being subjected to the standard firing cycle. Damage was observed with almost identical morphology to that seen in the laminates, confirming that damage can arise in laminates during densification even at tensile stresses of $\sim$1 MPa.

To further test the densification stress calculations, the theoretical approach was also used to predict the degree of curling and stresses that arise during the firing of asymmetric laminates. The results of the predicted curvature calculations are shown in Fig. 7 and are compared to the experimental measurements. The agreement between the theory and experiment is very good. For the asymmetric laminates, bending leads to a more complex stress distribution with tensile stresses occurring not in the zirconia layers (near the interface) but also in the outer alumina surface. Stresses up to $\sim$1·8 MPa were calculated for the alumina surface and in some laminates, cracking was observed at this location.[16]

4 Thermal Expansion Mismatch Stresses

The main difficulty in producing the alumina-zirconia laminates was the occurrence of transverse (channelling) cracks in the zirconia layers. Changing heating and cooling rates did lead to some differences in crack spacing but only the A100-Z70 system was found to be completely free of cracks[16]. It was initially assumed that these cracks were being formed primarily by the stresses that arise during cooling. Figure 8 shows the measured thermal expansion coefficients, α, for monoliths of the various layer types as a function of temperature, T. As the thermal expansion of zirconia is less than alumina, the zirconia layers will be placed in biax-

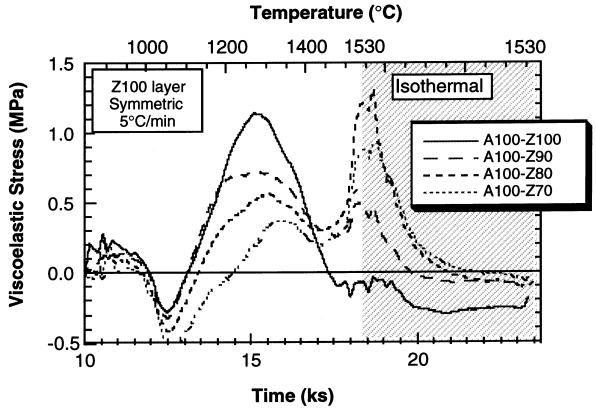

Fig. 6. Calculated viscoelastic stress in the ZrO_2-containing layers for the A100–Z100, A100–Z90, A100–Z80 and A100–Z70 symmetric laminates.

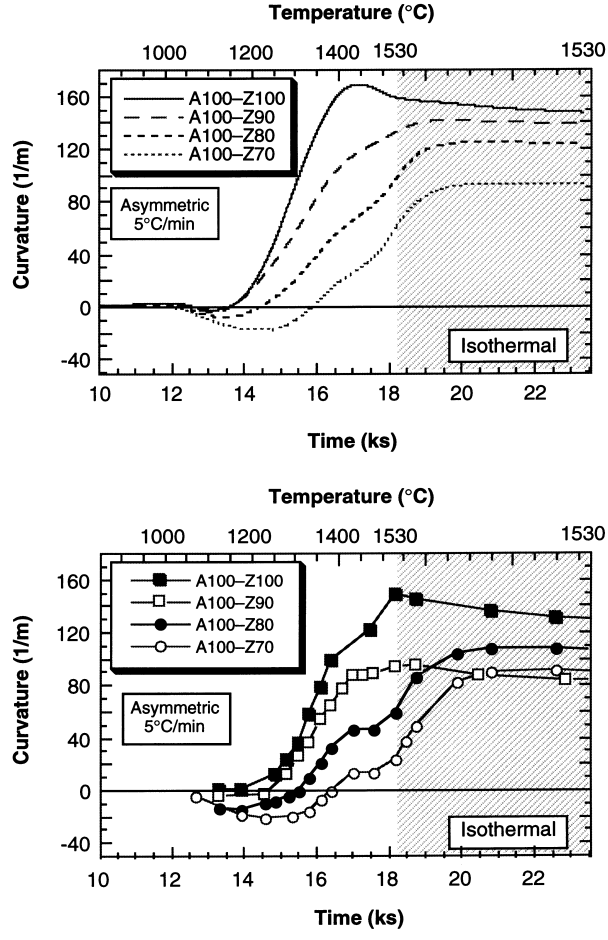

Fig. 7. Calculated and measured curvature for the A100–Z100, A100–Z90, A100–Z80 and A100–Z70 asymmetric laminates.

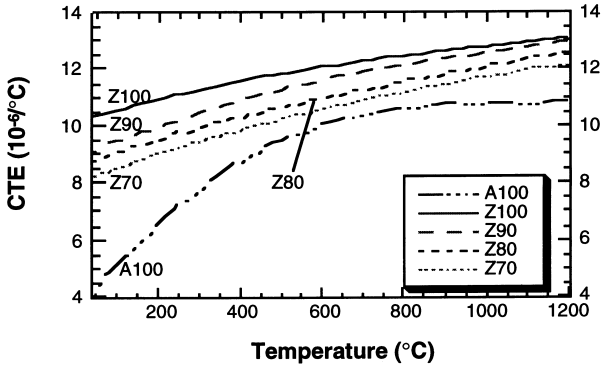

Fig. 8. Coefficients of thermal expansion (CTE) for A100, Z100, Z90, Z80 and Z70 measured by dilatometry.

ial tension. As expected, the alumina additions to the zirconia layers decrease the thermal expansion mismatch.

The elastic stresses in the layers that arise during cooling from the thermal expansion mismatch strain can be calculated from eqns. (2) and (3) by recognizing

$$\Delta e = \int_T (\alpha_2 - \alpha_1) \mathrm{d}T \tag{4}$$

It was assumed that these stresses start to arise once the temperature drops below 1200°C.[13] The results of the calculations are shown in Fig. 9 and stresses as high as 420 MPa were predicted. The addition of 30 wt% alumina dropped the stress to ~240 MPa. As indicated earlier, transverse cracking in these laminates can only occur if the layer thickness is above a critical value, t_c, given by[14]

$$t_c = \frac{4K_{IC}^2}{\pi\sigma_R^2} \tag{5}$$

where K_{IC} is the fracture toughness of the layer and σ_R is the residual stress. The decrease in the residual stress with the alumina addition increases the critical thickness by a factor ~3, making transverse cracking less likely for a fixed layer thickness. The value of the fracture toughness of the zirconia layer was determined to be 7·7 MPa$\sqrt{\text{m}}$.[18] For the A100–Z100 laminate, the critical thickness was calculated to be 430 μm. Since the actual layer thickness was ~120 μm, theoretically, the transverse cracking should not have occurred. One possible explanation, consistent with the earlier discussion, is that the linear damage incurred during densification effectively decreases the fracture toughness. The stresses that arise during cooling were also calculated from the viscoelastic data.[17] It was determined that changes in the cooling rate above 1200°C can influence the magnitude of these stresses and hence to some degree, can control the cracking behaviour.

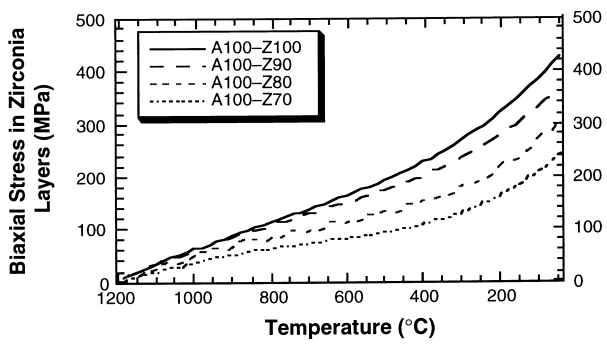

Fig. 9. Calculated biaxial thermal stresses during cooling in the ZrO_2 layer for the A100–Z100, A100–Z90, A100–Z80 and A100–Z70 symmetric laminates (elastic solution).

For the remainder of the paper, only the crack-free Z70–A100 laminate is discussed, though some changes were made in the laminate geometry. The base laminate system consisting of 120 μm thick Z70 and A100 layers was denoted as 1A–1Z. In the second system, the thickness of both layers were reduced by a factor of 2 (0·5Z–0·5A). In the last system, the zirconia layers were made twice as thick (1A–2Z). For the first two systems, the residual stress in the alumina layers was calculated to be −215 MPa and for the last system −430 MPa. By comparing the first two systems it was possible to determine whether interaction with the zirconia layer influenced the fracture toughness. The third system was chosen to show the effect of changing the residual stress.

In order to confirm the theoretically calculated residual stresses in the outer alumina layers, indentation crack lengths on the laminates were compared to those on monolithic alumina. It was assumed that the stress in the outer layers was uniform and that the indentation crack sizes were smaller than the layer thickness. For this situation, one can write[18]

$$\sigma_R = K_{IC} \frac{1 - (c_0/c_R)^{3/2}}{\psi\sqrt{c_R}} \tag{6}$$

where c_o and c_R are indentation crack length for the stress-free and stressed surfaces, respectively, and ψ is a geometric constant (~1·26). The results of this analysis are shown in Fig. 10 and good agreement is found between the stresses calculated from thermal expansion mismatch and change in indentation crack length. The main discrepancies are found for the thin layers at the higher loads, presumably because the indentation cracks had penetrated past the outer layer.

5 Effect of Residual Stress on Indentation Strength

If the outer layers are in residual compression, one expects an increase in indentation strength of the

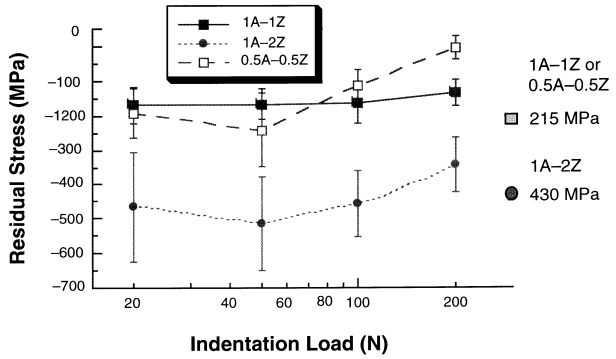

10. Calculated residual stress in the A100 surface layer using eqn. (6) for the 1A–1Z, 1A–2Z and 0·5A—0·5Z laminates. The data points on the right represent the calculated values from the measured coefficients of thermal expansion.

laminates compared to monolithic alumina when tested in flexure. This effect leads to an apparent increase in fracture toughness provided cracks initiate at the surface. Clearly, if this is the main strengthening mechanism for these laminates, it would not be very useful at high temperatures because the residual stresses will relax.

The indentation strength of a laminate, σ_f, can be calculated in a straightforward manner if it is again assumed that the stress in the outer layer is uniform and that the indentation crack sizes are smaller than the layer thickness. This approach gives [18]

$$\sigma_f = \left(\frac{\alpha K_{IC}^{4/3}}{P^{1/3}}\right) - \sigma_R \qquad (7)$$

where α is an indentation parameter. The indentation strength behaviour is shown in Fig. 11 and one can see the compressive stresses not only increase the indentation strength but also change the slope of the strength–load behaviour in this log–log plot. It is important to realize the stress values here are

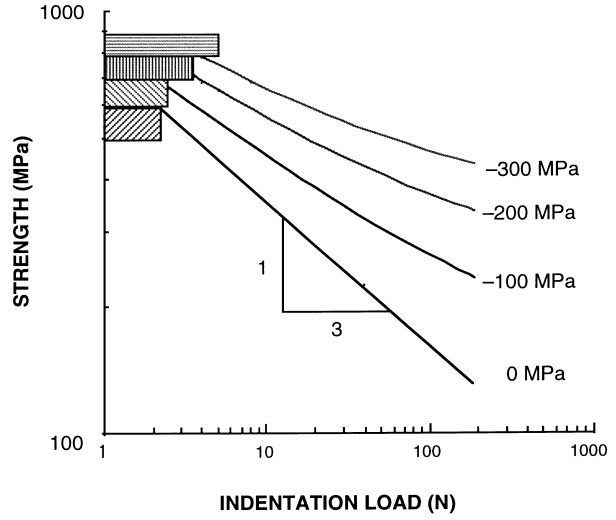

Fig. 11. Schematic showing the effect of a compressive residual surfaces stresses on indentation strength. The bars on the left represent the (non-indented) strength.

the actual values in the alumina layers. In the bend test, the elastic modulus of alumina is about a factor of two higher than zirconia. This leads to a modulation in the linear stress gradient normally associated with a flexure test. In particular, the stresses in the alumina were determined to be ~20% higher for the base laminate than nominal values calculated assuming the beam is homogeneous.[18] Figure 12 compares the nominal indentation strength data with that predicted by Eqn. (7) for the 1A–1Z and 0·5A–0·5Z laminates. The agreement is good even though there was evidence that the cracks interacted with the underlying layers, changing crack shape.[18] In particular, this effect appeared to influence the amount of stable crack growth on the tensile surface.

6 Conclusions

Significant residual stresses can arise in hybrid ceramic laminates during densification and cooling processing cycles. It is critical to understand the source of these stresses as this is not only one of the keys to successful processing but these stresses can also impact the mechanical performance. The differential densification stresses can be calculated assuming the layers are linear viscous and arise from the mismatch in sintering strain rates. Cyclic loading dilatometry is a useful technique to determine the viscous properties of ceramics that are required in the stress calculations. This dilatometric data showed a fairly sharp transition between elastic and viscous behaviour for the sintering compacts. For the laminates considered here, the densification stresses placed the zirconia layers in biaxial tension and even though the stress were 1 MPa or less, they were sufficient to cause a type of linear cavitation damage. This damage was also found to be preferred sites for the cracking that occurs during cooling. Additions of alumina

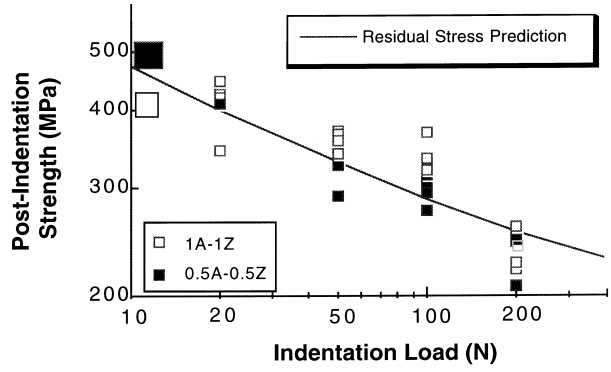

Fig. 12. Indentation strength of the 1A–1Z (open symbols) and 0·5A–0·5Z laminates (shaded). The line is drawn from eqn. (7) with a modulus correction[18]. The regions near the ordinate axis are the flexural strengths of the laminates.

to the zirconia layers was effective in reducing the densification stresses. More exact viscoelastic calculations were performed but these refinements made relatively small changes to the stress history. In order to confirm the stress values, the experimental approach was also applied to asymmetric composites and was successful in predicting the observed curling behaviour.

Higher stresses arise during cooling, placing the zirconia layers again in residual biaxial tension, leading to the formation of transverse (channelling) cracks. Additions of alumina to the zirconia layers was successful in reducing these stresses. Viscoelastic calculations showed these stresses could be reduced to some degree by reducing the cooling rate at temperatures $>1200°C$. The differential contraction stresses were also determined from indentation crack length measurements and good agreement was obtained with the theoretical calculations.

For bend testing of alumina–zirconia laminates at ambient temperatures, the thermal expansion mismatch stresses in the outer (alumina) layers led to an increase in indentation strength and an apparent decrease in the load exponent. This behaviour was shown to be consistent with theoretical considerations. The residual stresses also led to strengthening of the hybrid laminates.

References

1. Chan, H. M., Layered ceramics: processing and mechanical behaviour. In *Annual Review of Materials Science*, Vol. 27, ed. E. N. Kaufmann. Annual Reviews Inc., Palo Alto, CA. 1997.
2. Clegg, W. J., Kendall, K., Alford, N., Button, T. and Birchall, J. D., A simple way to make tough ceramics. *Nature*, 1990, **347**, 455–457.
3. Watkins, T. R. and Green, D. J., Fracture behaviour of CVD SiC-coated graphite: I. Experimental results. *J. Am. Ceram. Soc.*, 1992, **76**(12), 3066–3072.
4. Watkins, T. R. and and Green, D. J., Fracture behaviour of CVD SiC-coated graphite: II. Conditions for onset of multiple cracking. *J. Am. Ceram. Soc.*, 1993, **77**(3), 717–720.
5. Yttergren, R-M. F., Zeng, K. and Rowcliffe, D. J., Residual stress and crack propagation in laminated composites. In Ceramic Transactions, Vol 46, ed. J. P. Singh and N. P. Bansal. American Ceramic Society, Westerville, OH, 1994, pp. 543–553.
6. Wang, H. and Hu, X., Surface properties of ceramic laminates fabricated by die pressing. *J. Am. Ceram. Soc.*, 1996, **79**(2), 553–556.
7. Oechsner, M., Hillman, C. and Lange, F. F., Crack bifurcation in laminar ceramic composites. *J. Am. Ceram. Soc.*, 1996, **79**(7), 1834–1838.
8. Prakash, O., Sarkar, P. and Nicholson, P. S., Crack deflection in ceramic/ceramic laminates with strong interfaces. *J. Am. Ceram. Soc.*, 1995, **78**(4), 1125–1127.
9. Lakshminarayanan, R., Shetty, D. K. and Cutler, R. A., Toughening of layered ceramic composite with residual surface compression. *J. Am. Ceram. Soc.*, 1996, **79**(1), 79–87.
10. Kragness, E. D., Amateau, M. F. and Messing, G. L., Processing and characterization of laminated SiC whisker reinforced Al_2O_3. *J. Comp. Mater.*, 1991, **25**(4), 433–452.
11. Marshall, D. B., Ratto, J. J. and Lange, F. F., Enhanced fracture toughness in layered microcomposites of Ce-ZrO_2 and Al_2O_3. *J. Am. Ceram. Soc.*, 1991, **74**(12), 2979–2987.
12. Chen, Z. and Mecholsky, J. J., Toughening by metallic lamina in nickel/alumina composites. *J. Am. Ceram. Soc.*, 1993, **76** (5), 1258–1264.
13. Hillman, C., Suo, Z. and Lange, F. F., Cracking of laminates subjected to biaxial tensile stresses. *J. Am. Ceram. Soc.*, 1996, **79**(8), 2127–2133.
14. Ho, S. and Suo, Z., Tunnelling cracks in constrained layers. *J. Appl. Mech.*, 1993, **60**(4), 890–894.
15. Ho, S., Hillman, C., Lange, F. F. and Suo, Z., Surface cracking in layers under biaxial residual compressive stress. *J. Am. Ceram. Soc.*, 1995, **78**(9), 2353–2359.
16. Cai, P. Z., Green, D. J. and Messing, G. L., Constrained densification of Al_2O_3/ZrO_2 hybrid laminates: I. experimental observations. *J. Am. Ceram. Soc.*, 1997, **80**(8), 1929–1939.
17. Cai, P. Z., Green, D. J. and Messing, G. L., Constrained densification of Al_2O_3/ZrO_2 hybrid laminates: II. viscoelastic stress computation. *J. Am. Ceram. Soc.*, 1997, **80**(8), 1940–1948.
18. Cai, P. Z., Green, D. J., and Messing, G. L., Mechanical characterization of Al_2O_3/ZrO_2 hybrid laminates, *J. Eur. Ceram. Soc.*, 1998, **5**, 2025–2034.
19. Bordia, R. K. and Scherer, G. W., On constrained sintering—I. Constitutive model for a sintering body; and II. Comparison of constitutive models. *Acta Metall.*, 1988, **36**(9), 2393–2409.
20. Cai, P. Z., Messing, G. L. and Green, D. J., Determination of the mechanical response of sintering compacts by cyclic loading dilatometry. *J. Am. Ceram. Soc.*, 1997, **80**(2), 445–452.
21. Lam, D. C. C., Lange, F. F. and Evans, A. G., Mechanical properties of partially dense alumina produced from powder compacts. *J. Am. Ceram. Soc.*, 1994, **77**(8), 2113–2117.
22. Nanjangud, S. C., Brezny, R. and Green, D. J., Strength and Young's modulus behaviour of a partially sintered porous alumina. *J. Am. Ceram. Soc.*, 1995, **78**(1), 266–268.
23. Sglavo, V. M., Cai, P. Z. and Green, D. J., Damage in Al_2O_3 sintering compacts under very low tensile stress. *J. Mater. Sci. Letts.*, in press.